Abstract. In order to study whether there is any correlation between nuclear activities, gas content, and the environment where galaxies reside, we have obtained optical and millimetric spectra for a well-defined sample of intermediate Hubble type spirals in dense environments and in the field. We found that these spirals in dense environments have on average: less molecular gas per blue luminosity, higher atomic gas fraction, lower current star formation rate, and the same star formation efficiency as field galaxies. Although none of these results stand out as a single strong diagnostic, given their statistical significance, taken together they indicate a trend for diminished gas content and star formation activity in galaxies in high density environments. Our results suggest that galaxies in dense environments have either (i) consumed their molecular gas via star formation in the past or (ii) that dense environments leads to an inhibition of molecular gas from atomic phase. The similarities in star formation efficiency of the dense environments and field galaxies suggest that the physical processes controling the formation of stars from the molecular gas are local rather than global. We also found that star formation rate per blue luminosity increases linearly as the total amount of gas increases in LINERs. This result, based on a small sample, suggests that LINERs are powered by star formation rather than an AGN.

Environmental effects in galaxies

Molecular Gas, Star Formation, and Activity[*]

Duilia F. de Mello[1] Tommy Wiklind[1] and Marcio A. G. Maia[2]

[1] Onsala Space Observatory, 43992 Onsala, Sweden
   email: duilia@oso.chalmers.se, tommy@oso.chalmers.se
[2] Observatório Nacional, Rua Gal. José Cristino 77, RJ 20921, Brazil
   email: maia@on.br

1. Introduction

The importance of interactions for triggering activity in galaxies has been extensively explored in the past few decades (e.g. Larson & Tinsley 1978, Dahari 1984, Kennicutt & Keel 1984, Keel et al. 1985, Mihos & Hernquist 1994, Liu & Kennicutt 1995, Keel 1996). There is no doubt that the environment where galaxies reside plays a decisive role in galaxy evolution. Nevertheless, there are a few key questions which are still being debated. For instance, the environmental influences on the star formation properties of clusters of galaxies is far from clear-cut. Although the molecular gas properties of strongly HI deficient spirals in the Virgo cluster is similar to field spirals (Kenney & Young 1988), the average star formation activity among them are lower than for a sample of field spirals (Kennicutt 1983). This latter effect is, however, not seen in the Coma, Cancer, and A1367 clusters, where star formation activity appears to be enhanced with respect to field spirals (Kennicutt et al. 1984). The Coma spirals are similar to those in the Virgo cluster: deficient in atomic gas, while the molecular gas properties are the same as for field spirals (Casoli et al. 1991, 1996; Gerin & Casoli 1994). In the Fornax cluster, Horellou et al. (1995) found no evidence for HI deficiency, but an unusual low fraction of molecular gas. For galaxies in loose groups, Maia et al. (1998) find only weak evidence for HI depletion in the early-type spirals.

In compact groups of galaxies the environmental role is also an open issue. Compact groups of galaxies are longlived entities with a space density of galaxies higher than in clusters (see Hickson 1997 for a review). Triggering of star formation through gravitational interaction should therefore be even more important in this environ-

ment, but the results indicate differently. Even though compact groups present a high fraction of distorted galaxies (Mendes de Oliveira & Hickson 1994), they do not show an enhancement in far-infrared (FIR) emission (Sulentic & de Mello Rabaça 1993, Allam et al. 1996), they have low HI content (Williams & Rood 1987, Huchtmeier 1997), and a normal CO content (Boselli et al. 1996, Leon et al. 1998).

In pairs of galaxies, the scenario is different. The CO and far–infrared luminosities, normalized with either the size of the respective galaxy or L_B, is enhanced (Combes et al. 1994). However, whereas the star formation efficiency (SFE = star formation rate per mass unit of molecular gas) is higher in pairs which are strongly interacting/merging, the average SFE of the whole sample of pairs is similar to normal field spirals. A possible interpretation is that gravitational interactions do not increase the SFE, but increases the amount of star forming gas, possibly through infall of new material.

It has been shown that strong gravitational interactions between galaxies can enhance the star formation rate (SFR) (e.g. Liu & Kennicutt 1995). It has also been proposed that it is the near environment that mostly affects the evolution of galaxies (Szomoru et al. 1996). However, the connection between the environment, nuclear activities and total gas content has not been able to explain which variables are important in deciding how efficient stars are formed. Are galaxies in dense environments more efficient in forming stars or do they have more fuel? How is the star formation efficiency correlated with the environment where galaxies reside? Is the near environment that mostly affects the evolution of galaxies. An essential step towards answering these open questions is to compare the properties of galaxies in dense environments and in the field.

In this work we present the analysis of the data shown in de Mello et al. (2001, hereafter Paper I) which is a database of molecular and optical spectra of galaxies in dense regions of the Southern sky and in the field.

This paper is organized as follows. Section 2 presents the diagnostics used in this work. Discussion is presented in Section 3 and a summary of the main results and conclusions are presented in Section 4.

2. Diagnostics

Optical and millimetric data have been obtained with the ESO1.52m and the SEST 15m radio telescope in la Silla, Chile and we refer to Paper I for further details. Table 1 lists the data as follows. Column (1): designation in the ESO-Uppsala catalog (Lauberts & Valentijn 1989, hereafter LV89); column (2): type of sample (control sample=CS and high density sample=HDS) and morphological type (LV89) 1=Sa, 2=Sa-b, 3=Sb, 4=Sb-c, 5=S..., 6=Sc, Sc-d, 7=S../Irr, 8=Sd; column (3): velocity derived from central CO (1-0) profiles in kms^{-1}; column (4): distance in Mpc corrected for the Virgocentric flow according to model 3.1 in Aaronson et al. (1982); column (5): blue luminosity in L$_\odot$ derived from B$_T$ magnitude taken from RC3; column (6): HI masses in M$_\odot$ derived using the relation M$_{HI}$ = $2.36 \times 10^5 \times$ D$^2 \times$ F(HI), where M$_{HI}$ is the HI mass in M$_\odot$, D is the distance in Mpc, and F(HI) is the HI flux in Jy kms^{-1} taken from the NASA/IPAC Extragalactic Database (NED) (blank = no HI data available); column (7): Far-Infrared luminosity in L$_\odot$ calculated from L$_{FIR}$ = 5.9×10^5D^2($2.58 \times$F$_{60}$+F$_{100}$) where D is the distance in Mpc and F are IRAS fluxes at 60 and 100 μm (Moshir et al. 1990); column (8): H$_2$ masses in M$_\odot$ estimated from the velocity integrated emission, using a N$_{H_2}$/I$_{CO}$ conversion ratio of 3×10^{20} cm^{-2} (K kms^{-1}); column (9): dust temperature in K calculated as described in Sect. 2.3; column (10): dust masses in M$_\odot$ calculated as described in Sect. 2.3; and column (11): type of activity (L = LINERs, HII = HII region, blank = no optical data) classified as described in Sect. 2.2. A Hubble constant value of 75 kms^{-1}Mpc^{-1} was adopted in all calculations.

The diagnostics used in our search for environmental effects are summarized in Table 2 and Table 3. Due to the presence of galaxies with higher L$_B$ in the CS (a distance bias in our subsample), masses and luminosities were normalized by L$_B$. Given our morphological selection criteria, we assumed that the mass/L$_B$ ratio is approximately the same for our galaxies and L$_B$ is thus a measure of the total mass (e.g. Roberts & Haynes 1994). In Fig. 3a of Paper I we have investigated whether the bias in blue luminosity present in our subsample may cause a bias in our analysis. The correlation found for HDS and CS when we plotted M$_{H_2}$/L$_B$ as a function of L$_B$ is very similar suggesting no evident bias.

We included in Table 2 the average values given by Leon et al. (1998) for pairs of galaxies, Hickson Compact Groups, starbursts and clusters. We have also included the average values from Leon et al. for galaxies in compact groups using the same morphological criterion we used in our selection (Sb, Sbc, and Sc).

The distributions of the diagnostics are shown in Fig. 1. The cumulative distributions are shown in Fig 2. The distribution of morphological types for the HDS and the CS were also included in order to verify how similar the two samples were in terms of morphology. This is a very important aspect to be considered in this type of analysis since morphological appearance is directly correlated with general properties of galaxies. We refer to Section 2.4 of Paper I for more details on our morphology selection and to Roberts & Haynes (1994) for a review on physical parameters along the Hubble sequence.

The significance of the small difference between the mean values of the HDS and the CS was assessed using the Student-t test for unequal variances. The Kolmogorov-Smirnov statistics (KS, hereafter) was used to assess the significance level of the difference between the cumulative distributions. Table 4 shows: column (1) the value of KS (same as D in Press et al. 1989), which is the greatest distance between two cumulative distributions in the KS statistics; column (2) the significance level KS$_{Pb}$; column (3) the Student-t coefficient T for unequal variances; and column (4) the significance level T$_{Pb}$. Small values of T$_{Pb}$ indicate that the distributions have significantly different means. Small values of KS$_{Pb}$ indicate that the cumulative distribution of the HDS is significantly different from that of the CS. The main results are:

- The HDS and the CS have similar morphology distribution.
- The HDS has on average lower M$_{H_2}$/L$_B$ than the CS. M$_{H_2}$/L$_B$ distributions are significantly different. Their means differ at the 93% level.
  Therefore, *HDS spirals have overall less molecular gas per blue luminosity than spirals in the field.*
- The HDS has on average lower L$_{FIR}$/L$_B$ than the CS. L$_{FIR}$/L$_B$ distributions are different at the 67% level. Their means differ at the 84% level.
  Therefore, *the HDS spirals have, on average, lower L$_{FIR}$/L$_B$ than the CS.*
- The L$_{FIR}$/M$_{H_2}$ ratio can be interpreted as a measure of the star formation efficiency (star formation rate per unit mass of molecular gas). The HDS has on average higher L$_{FIR}$/M$_{H_2}$ than the CS. However, the level of significance given by the Stundent-t test and KS statistics is only at the 60% and 57% level.
  Therefore, *the star formation efficiency in the HDS is not statistically different than in the CS.*

2.1. Comparing with other samples

We showed in Paper I that our subsamples of the HDS and the CS have general properties, such as FIR luminosity, blue luminosity, and molecular gas content, very similar to other galaxies such as normal spiral galaxies (Young et al. 1989, Braine et al. 1993), ultraluminous FIR galaxies (Sanders et al. 1991), and galaxies in the Coma and Fornax

Table 1. The Data

ESO-LV Name (1)	Sample & Morph. (2)	V_{CO} kms^{-1} (3)	Dist. Mpc (4)	$\log L_B$ $L_\odot$ (5)	$\log M_{HI}$ $M_\odot$ (6)	$L_{FIR} \times 10^9$ $L_\odot$ (7)	$M_{H_2} \times 10^9$ $M_\odot$ (8)	T_{dust} K (9)	$M_{dust} \times 10^6$ $M_\odot$ (10)	Type of Activity (11)
0310050	CS 3.5	4714	59.2	10.11		13.60 ± 0.39	3.30 ± 0.23	28.64 ± 0.49	9.98 ± 0.95	HII
1060120	CS 6	4154	52.0	9.97		6.90 ± 0.39	1.93 ± 0.19	29.45 ± 1.03	4.24 ± 0.81	HII
1080130	HDS 3.5	2941	35.8	9.78		2.67 ± 0.15	0.81 ± 0.07	28.91 ± 1.00	1.85 ± 0.35	HII
1080200	CS 3.9	1719	19.9	9.37	9.63	4.45 ± 0.20	0.65 ± 0.03	28.71 ± 0.82	3.22 ± 0.49	
1190060	HDS 7.5	1256	14.4	9.48	8.91	1.66 ± 0.05	0.11 ± 0.01	32.62 ± 0.72	0.55 ± 0.06	
1190190	HDS 5	1527	18.0	9.94	9.14	2.52 ± 0.07	0.42 ± 0.02	28.85 ± 0.50	1.77 ± 0.17	HII
1420500	CS 5	2135	25.9	10.10	9.98	4.40 ± 0.09	0.59 ± 0.04	28.78 ± 0.44	3.12 ± 0.24	L
1460090	CS 5	1652	19.0	10.131	9.47	10.40 ± 0.34	1.10 ± 0.06	30.88 ± 0.70	4.75 ± 0.51	HII
1570050	HDS 5.5	1326	15.2	9.30	8.84	0.39 ± 0.02	0.10 ± 0.01	29.27 ± 0.96	0.25 ± 0.05	HII
1890070	CS 4.0	3006	36.7	10.44		9.15 ± 0.36	1.48 ± 0.09	31.74 ± 0.83	3.54 ± 0.46	
2010220	CS 5	3990	50.1	9.70	9.90	3.53 ± 0.23	0.98 ± 0.07	27.81 ± 1.03	3.14 ± 0.67	HII
2030180	CS 4	4123	52.2	10.27		25.39 ± 1.17	3.30 ± 0.16	32.28 ± 1.02	8.88 ± 1.41	HII
2340160	HDS 5	5218	66.4	10.01		3.72 ± 0.50	0.94 ± 0.06	32.22 ± 3.00	1.32 ± 0.63	HII
2350550	HDS 5	5098	64.6	10.73		9.92 ± 1.11	2.04 ± 0.12	24.89 ± 1.22	8.61 ± 6.00	L
2350570	HDS 4	5069	64.2	10.03		11.08 ± 1.30	3.45 ± 0.13	23.83 ± 1.23	8.20 ± 9.77	L
2370020	CS 4.5	5173	65.3	10.58	10.21	13.72 ± 0.70	4.90 ± 0.18	27.44 ± 0.78	3.31 ± 2.20	L
2400110	HDS 4.8	2890	34.9	10.00	10.26	5.81 ± 0.31	1.65 ± 0.05	25.20 ± 0.93	9.98 ± 2.16	L
2400130	HDS 3	3284	40.1	9.80		5.17 ± 0.31	1.08 ± 0.06	27.44 ± 0.85	5.02 ± 0.94	
2850080	HDS 4	2838	35.3	10.63	10.34	4.45 ± 0.23	0.64 ± 0.07	26.69 ± 0.74	5.18 ± 0.86	L
2860820	HDS 5	4958	62.8	9.98		4.42 ± 0.51	1.66 ± 0.09	30.44 ± 2.23	2.21 ± 0.87	HII
2880260	HDS 5	2383	28.8	9.79	9.57	1.42 ± 0.10	0.32 ± 0.02	29.40 ± 1.29	0.88 ± 0.21	L
2960380	CS 4	3645	45.1	9.90		3.73 ± 0.33	0.44 ± 0.06	29.33 ± 1.69	2.35 ± 0.72	HII
3050140	CS 5	4761	61.1	10.11	9.78	4.31 ± 0.55	2.31 ± 0.10	32.15 ± 2.80	1.55 ± 0.71	HII
3470340	HDS 3	1671	19.3	9.92	9.70	7.85 ± 0.79	2.27 ± 0.06	28.00 ± 1.54	6.67 ± 2.14	
3500140	CS 6	3400	42.0	10.09	9.73	3.30 ± 0.25	1.23 ± 0.04	30.04 ± 1.49	1.79 ± 0.47	HII
3520530	HDS 3	3874	48.2	10.27	9.20	21.89 ± 0.93	6.55 ± 0.32	30.53 ± 0.83	0.75 ± 1.54	
3550260	CS 4	1985	23.8	9.42	8.82	0.95 ± 0.07	0.15 ± 0.02	29.75 ± 1.46	0.55 ± 0.14	
3550300	CS 4	4448	56.1	10.25	9.82	10.05 ± 0.43	3.33 ± 0.36	29.04 ± 0.75	6.75 ± 0.96	L
3570190	HDS 5	1789	21.4	9.83	9.43	1.52 ± 0.06	0.41 ± 0.03	28.48 ± 0.67	1.15 ± 0.15	HII
4050180	CS 1	3375	41.9	10.27	8.87	10.67 ± 0.68	3.52 ± 0.17	33.19 ± 1.50	3.17 ± 0.70	
4060250	HDS 5	1470	16.9	9.98	9.26	4.42 ± 0.20	2.04 ± 0.05	29.31 ± 0.83	2.80 ± 0.43	
4060330	HDS 6	1922	22.8	9.71	9.72	5.01 ± 0.21	0.42 ± 0.02	31.61 ± 0.90	1.99 ± 0.29	HII
4070140	CS 5	2761	33.6	9.85	9.54	3.54 ± 0.23	0.78 ± 0.04	31.34 ± 1.33	1.48 ± 0.33	HII
4190030	CS 4	4146	52.8	10.20	9.82	11.19 ± 0.36	1.10 ± 0.09	32.48 ± 0.71	3.77 ± 0.42	HII
4200030	CS 5	4093	52.2	10.22	9.83	6.41 ± 0.41	2.02 ± 0.14	30.37 ± 1.24	3.25 ± 0.70	HII
4710200	CS 4.5	3017	37.0	10.30	10.17	12.49 ± 0.53	1.95 ± 0.13	30.08 ± 0.81	6.72 ± 0.96	HII
4780060	CS 4	5401	68.9	10.58	9.95	51.12 ± 2.91	10.86 ± 0.4	32.26 ± 1.26	7.96 ± 3.55	HII
4820430	CS 4	4073	51.9	10.17	9.74	6.57 ± 0.33	2.35 ± 0.21	26.86 ± 0.81	7.33 ± 1.27	HII
4840250	CS 2	4128	53.0	10.13		16.54 ± 0.64	2.65 ± 0.22	32.17 ± 0.85	5.90 ± 0.79	
5320090	CS 5	2582	32.0	9.91	9.31	4.22 ± 0.20	0.41 ± 0.05	31.61 ± 0.98	1.67 ± 0.26	HII
5390050	CS 5	3158	39.4	9.98	8.99	5.03 ± 0.29	1.99 ± 0.13	30.51 ± 1.11	2.48 ± 0.47	HII
5450100	HDS 5	1715	20.9	9.55	9.07	3.21 ± 0.14	0.15 ± 0.01	34.52 ± 1.08	0.76 ± 0.11	HII
5450110	HDS 5	1456	17.5	10.35	9.60	14.78 ± 0.72	2.15 ± 0.07	30.79 ± 0.91	6.88 ± 1.14	
5480070	HDS 3.5	1557	19.2	9.87	9.38	1.05 ± 0.05	0.17 ± 0.01	26.19 ± 0.80	1.39 ± 0.25	
5480310	HDS 3	1531	18.9	9.79	8.60	3.17 ± 0.13	0.65 ± 0.03	28.87 ± 0.79	2.21 ± 0.31	L
5480380	HDS 6	1874	23.3	10.03	9.23	10.56 ± 0.31	0.30 ± 0.02	41.99 ± 1.08	0.87 ± 0.09	HII
6010040	CS 4.6	5219	66.8	10.01	9.73	3.85 ± 0.56	1.17 ± 0.09	28.33 ± 2.74	3.03 ± 1.57	HII

CS=control sample and HDS=high density sample; morphological types are 1=Sa, 2=Sa-b, 3=Sb, 4=Sb-c, 5=S..., 6=Sc, Sc-d, 7=S./Irr, 8=Sd. Column(11): HII=activity typical of HII regions, L=LINERs, blank means no optical data. † M_{H_2} of 5 points along the major axis. ‡ M_{H_2} of 7 points along the major axis.

clusters (Casoli et al. 1991 and Horellou et al. 1995); i.e. they are not a separate class of objects.

However, our M_{H_2}/L_B average value ($\log(M_{H_2}/L_B)$= -0.91 ± 0.24 for the CS) is lower than the classical value from Young & Knezek (1989) ($\log(M_{H_2}/L_B) \sim -0.77 \pm 0.05$ $M_\odot/L_\odot$). The main reason for this disagreement is that Young & Knezek sample of spirals was FIR-selected, it is biased towards higher L_{FIR} and therefore towards

Table 2. Diagnostic Quantities

Sample[†]	log (L_{FIR}/M_{H_2}) $L_\odot/M_\odot$	log (M_{H_2}/L_B) $M_\odot/L_\odot$	log (L_{FIR}/L_B) $L_\odot/M_\odot$	log $(M_{H_2}+M_{HI}/L_B)$ $M_\odot/L_\odot$	log $(L_{FIR}/M_{H_2}+M_{HI})$ $L_\odot/M_\odot$	T_D K	log (M_D/L_B) $M_\odot/L_\odot$
HDS	0.74 ± 0.31	-1.09 ± 0.39	-0.35 ± 0.32	-0.35 ± 0.29	-0.01 ± 0.42	31.3 ± 2.8	-3.65 ± 0.27
CS	0.67 ± 0.21	-0.91 ± 0.24	-0.24 ± 0.22	-0.27 ± 0.25	0.00 ± 0.26	30.1 ± 2.4	-3.48 ± 0.30
Pairs	0.91 ± 0.43	-0.57 ± 0.45	0.33 ± 0.48	-0.47 ± 0.31	1.04 ± 0.37	34.9 ± 6.0	-3.37 ± 0.40
HCG	0.39 ± 0.33	-0.61 ± 0.39	-0.16 ± 0.45	-0.42 ± 0.22	-0.02 ± 0.40	33.1 ± 5.7	-3.42 ± 0.36
HCG$_{int.type}$	0.37 ± 0.40	-0.66 ± 0.35	-0.29 ± 0.49	-0.14 ± 0.31	-0.12 ± 0.40	32.3 ± 5.6	-3.41 ± 0.32
Starbursts	1.24 ± 0.39	-0.61 ± 0.43	0.63 ± 0.43	-0.36 ± 0.40	0.91 ± 0.39	40.4 ± 6.2	-3.27 ± 0.34
Clusters	0.77 ± 0.37	-1.08 ± 0.36	-0.31 ± 0.40	-0.73 ± 0.34	0.42 ± 0.35	33.2 ± 4.7	-3.78 ± 0.30

[†] HDS is our high density sample, CS is our control sample of isolated galaxies, Pairs, Hickson Compact Groups (HCG), Starbursts and Clusters are from Leon et al. (1998). HCG$_{int.type}$ are HCG galaxies of types Sb, Sbc, and Sc in Leon et al (1998).

Table 3. Correlation Coefficients

Diagnostic	r HDS	r CS
$L_{FIR} \times M_{H_2}$	0.80	0.84
$L_B \times M_{H_2}$	0.64	0.78
$L_{FIR}/L_B \times M_{H_2}/L_B$	0.65	0.59
$L_{FIR}/L_B \times L_{FIR}/M_{H_2}$	0.21	0.36
$T_D \times L_{FIR}/M_{H_2}$	0.63	0.27
$T_D \times M_{H_2}/M_D$	0.56	0.44
$L_{FIR}/L_B \times L_{FIR}/(M_{H_2}+M_{HI})$	0.73	0.46

Table 4. Statistical Values

Diagnostic	KS	KS$_{Pb}$	T	T$_{Pb}$
Morphology	0.20	0.74	-0.52	0.60
log (M_{H_2}/L_B)	0.33	0.16	-1.89	0.07
log (L_{FIR}/L_B)	0.28	0.33	-1.43	0.16
log (L_{FIR}/M_{H_2})	0.23	0.57	0.85	0.40
log (M_{HI}/L_B)	0.31	0.42	0.45	0.65
log $(M_{H_2}+M_{HI}/L_B)$	0.42	0.09	-1.19	0.24
log $(L_{FIR}/M_{H_2}+M_{HI})$	0.27	0.55	0.16	0.87
log (M_{HI}/M_{H_2})	0.40	0.12	0.87	0.39
T_D	0.28	0.33	-0.63	0.54

KS is the greatest distance between two cumulative distributions in the Kolmogorov-Smirnov statistics. KS$_{Pb}$ is the significance level to the null hypothesis that the data sets are drawn from the same distibution. T is the Student t coefficient for unequal variances and T$_{Pb}$ is the significance level.

Fig. 3. Diagnostic diagram - log([OIII]$\lambda5007/H\beta$) versus log([NII]$\lambda6583/H\alpha$). Solid lines divide the nuclear activities in Seyferts, LINERS, HII galaxies, based on Veilleux & Osterbrock (1987). The CS is marked by open squares. The HDS is marked by solid circles.

higher M_{H_2}. A sample like CS which is not selected with any FIR limit, is more realistic for the field.

Another sample of isolated galaxies such as the one used in Leon et al. (1998) shows a high dispersion of log$(M_{H_2}/L_B) \sim -0.78 \pm 0.58$ M$_\odot$/L$_\odot$ which demonstrates that their sample is not very homogeneous in terms of molecular gas content. This is due to the fact that the sample of Leon et al. (1998) includes all morphological types, whereas our sample has only galaxies Sb, Sbc, and Sc. This is also seen when one compares Hickson Compact Groups of all types with HCG later than Sa and earlier than Sd given in Table 2.

2.2. Nuclear Activity

It is believed that one of the environmental effects in disk systems is the efficient transport of gas to the centers of
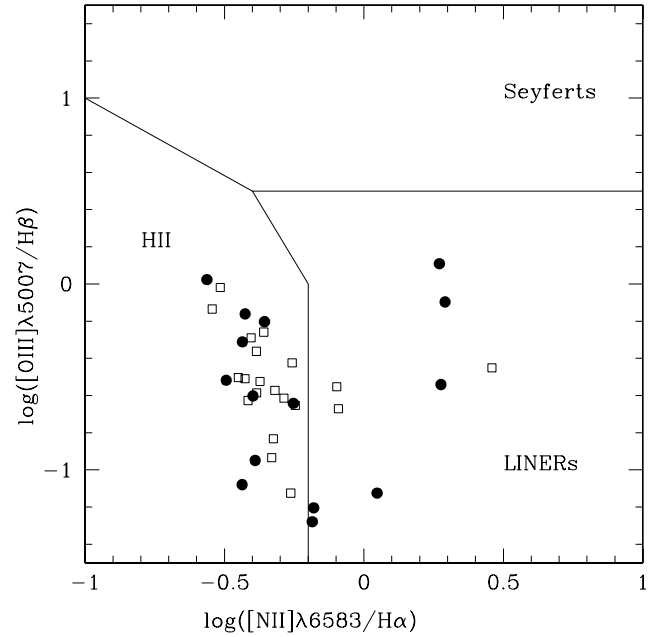
the galaxies caused by gravitational interaction. This process can in principle trigger nuclear thermal (starbursts) and nonthermal activities (AGNs). The classification of the type of activity in our sample was done by measuring line-intensity ratios and applying standard diagnostic diagrams (Baldwin et al. 1981, Veilleux & Osterbrock 1987). Fluxes have been corrected for galactic and internal reddening. However, due to the close wavelength separation of the lines used in the ratios, the internal reddening correction is nearly negligible. In Fig. 3 we show the log([OIII] λ 5007/Hβ) versus log([NII] λ 6583/Hα) for 35 galaxies (15 in the HDS and 20 in the CS). Most of the galaxies have spectra showing signs of star formation (HII-type). A total of 9 LINERs were identified, 3 in the CS and 6 in the HDS. Field spiral galaxies and close pairs of galaxies are reported in the literature to have 19% and 10% of LINERs (Ho et al. 1997 and Barton et al. 2000).
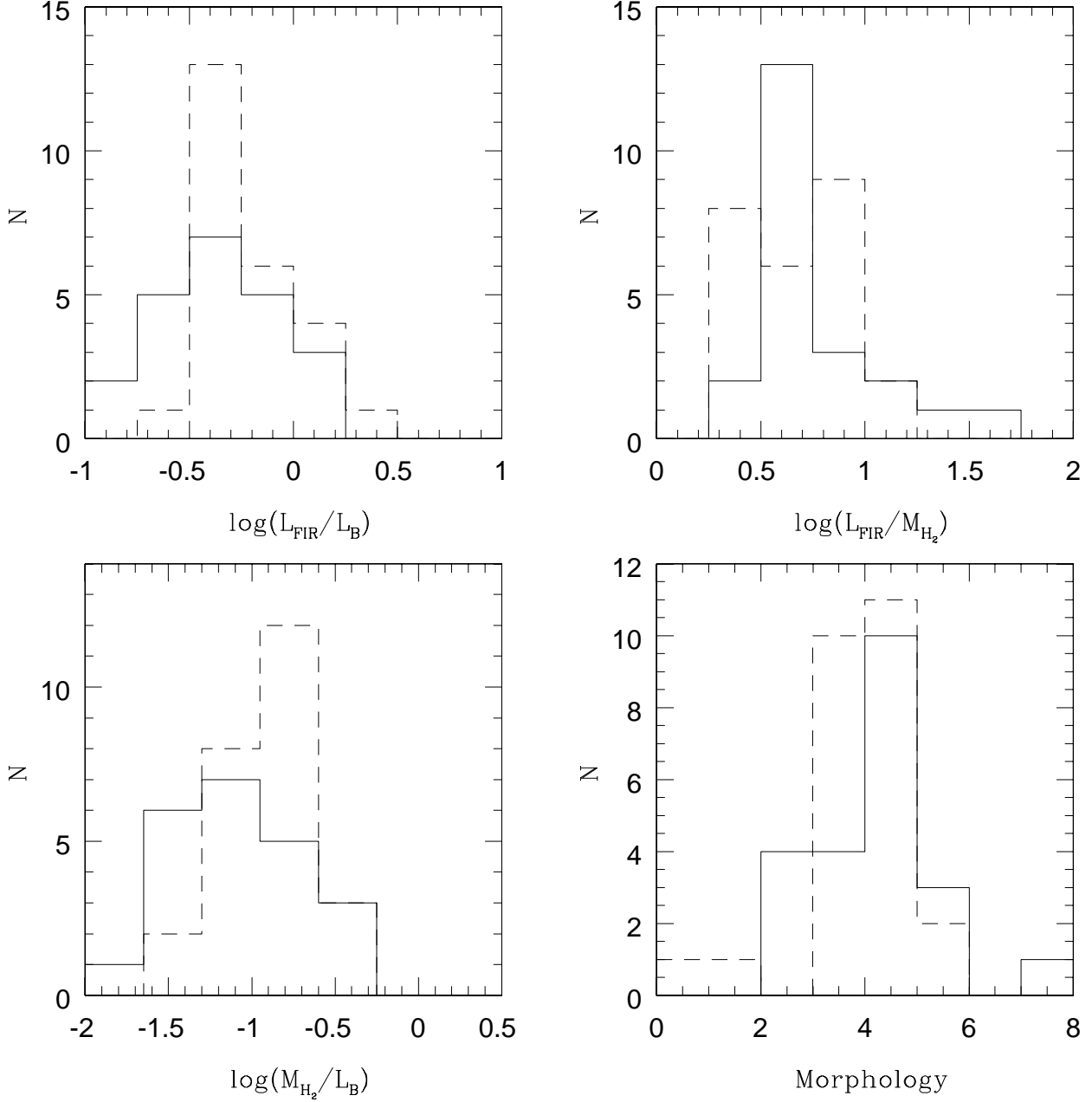
Fig. 1. Upper left panel: Distribution of FIR luminosity normalized by blue luminosity; Upper right panel: Distribution of FIR luminosity normalized by molecular gas; Lower left panel: Distribution of molecular gas normalized by blue luminosity; Lower right panel: Distribution of morphological types. Morphological types are: 1=Sa, 2=Sa-b, 3=Sb, 4=Sb-c, 5=S..., 6=Sc, Sc-d, 7=S../Irr, 8=Sd. Full line is for the HDS and dashed line is for the CS. Luminosities are in $L_\odot$, mass in $M_\odot$.

The lack of Seyfert galaxies in our subsample seems to be in disagreement with the recent work by Coziol et al. (2000) who reported a high number of Seyfert galaxies in compact groups of galaxies. However, whereas our HDS subsample includes only intermeditate spiral galaxies, their sample includes both early- and late-type galax-

ies, with the Seyferts being more common in earlier types (E and S0s). However, intermediate type spirals can also host AGNs. For example, in the work by Maiolino et al. (1997) where they studied the molecular gas content of 94 Seyfert galaxies, there are 43 spirals of intermediate types. Therefore, the lack of Seyferts in our subsamples
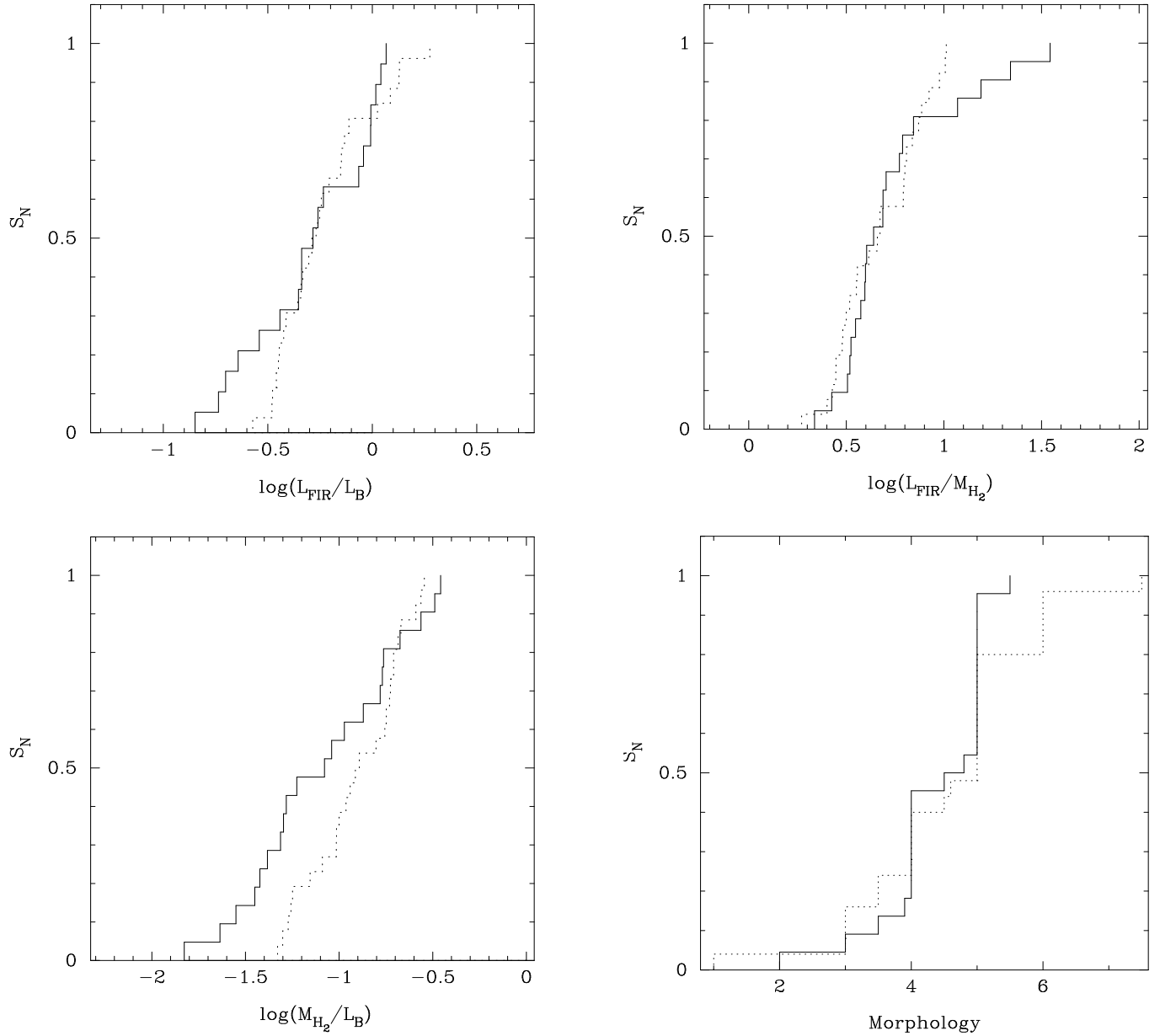
Fig. 2. Cumulative probability distribution of the same parameters of Fig. 1.

could be either due to a bias in our classification of activities or to the size of our small subsample. The fact that we used $H\alpha/H\beta=2.86$ in some galaxies where it was not possible to measure $H\beta$ in emission will not change the the diagnostic diagram significantly. For instance, if we use $H\alpha/H\beta=3.1$ (typical of AGNs) instead of $H\alpha/H\beta=2.86$, the change in the vertical axis will not be large enough to bring the data points into the Seyfert regions. Therefore, the lack of Seyferts in our subsample can be explained by our morphology selection and by the small number of galaxies in or subsample.

Fig. 4 shows the correlation between the total molecular gas, M_{H_2}, and L_{FIR}, both divided by L_B. The correlation coefficient is 0.65 and 0.59 for the HDS and CS.

However, if we consider only LINERs, the correlation coefficient increases to 0.99 and 0.75; i.e. the star formation rate (SFR) per blue luminosity increases linearly as the total amount of molecular gas increases in LINERs, in particular for the HDS. This result might have important implications in the understanding of the nature of LINERs (e.g. Alonso-Herrero et al. 2000). However, a larger sample of LINERs should be used in order to statistically test the significance of this trend. Another interesting result is the fact that the galaxies which deviates from the linear correlation are all non-AGN galaxies. Hence, AGN heating of dust cannot be invoked as an explanation for the higher L_{FIR}/L_B for a given M_{H_2}/L_B.

Table 5. T_D and SFE average values

Diagnostic	LINERs		Non-LINERs	
	HDS	CS	HDS	CS
T_D	26.5±2.3	28.4±0.8	31.3 ±2.8	30.1 ±2.4
log L_{FIR}/M_{H_2}	0.65±0.12	0.60±0.23	0.77±0.35	0.68±0.21

2.3. Dust temperature

Dust temperature can provide a better understanding of the physical conditions inside the galaxies. Warm dust ($T_D > 50$ K) are typical of molecular clouds where massive stars (> 6 $M_\odot$) reside, whereas cold dust ($T_D < 30$ K) trace quiescent molecular clouds heated by the interstellar radiation field. However, the limited spatial resolution of IRAS gives an average of extended cold dust emission and small hot emission areas (the dust emissivity goes as T_D^4). Nevertheless, a higher dust temperature is indicative of current star formation. From the ratio of the IRAS fluxes at 60 μm and 100 μm we derived dust temperatures assuming $\kappa_\nu \propto \nu$. Dust masses were derived using the following equation,

$$M_D = 4.8 \times 10^{-11} \alpha S_{100} d^2/(\kappa_\nu B_\nu (T_D))$$

where S_{100} is the IRAS flux at 100 μm in Jy, κ_ν is the mass opacity of the dust (κ_ν=25 cm^{2}g^{-1}, Hildebrand 1983), $B_\nu(T_D)$ is the Planck function, d is the distance in Mpc, and α the molecular gas-to-dust mass ratio (α=700, Thronson & Telesco 1986).

The average values of T_D (HDS=31.3 ± 2.8 and CS=30.1 ± 2.4) are typical of spiral galaxies (Sage 1993, Wiklind et al. 1995). In Fig. 5 we see that there is a lack of correlation between SFE and T_D for the CS and a weak correlation for the HDS (correlation coefficients are ~ 0.3 and 0.6, respectively). However, the relatively low values of T_D for LINERs (Table 5) might have important implications regarding the interpretation of the source that powers the nuclear region of these galaxies. Low T_D implies a low current star formation and no powerful black hole. The scenario proposed by Alonso-Herrero et al. (2000) fits well our results. If LINERs are aging starbursts they should have low T_D since their massive stars would have evolved after 5–10 Myr. This is also suggested by the lower averages of log L_{FIR}/M_{H_2} for LINERs. However, we cannot exclude the presence of a central black hole with reduced activity (Ji et al. 2000). In view of the small number of LINERs in our sample it is not possible to reach any firm conclusion regarding the correlation between the amount of fueling gas and the starburst and/or AGN activities.

2.4. Star Formation Rate

The Hα equivalent width (EW) is defined as the emission-line luminosity normalized to the adjacent continuum flux, and hence is proportional to the star formation rate per unit (red) luminosity. The mean value of EW(Hα) for the HDS and CS are 14.9 ± 11.7 and 13.4 ± 9.5 Å, respectively. These values are lower than the ones found in Pas-
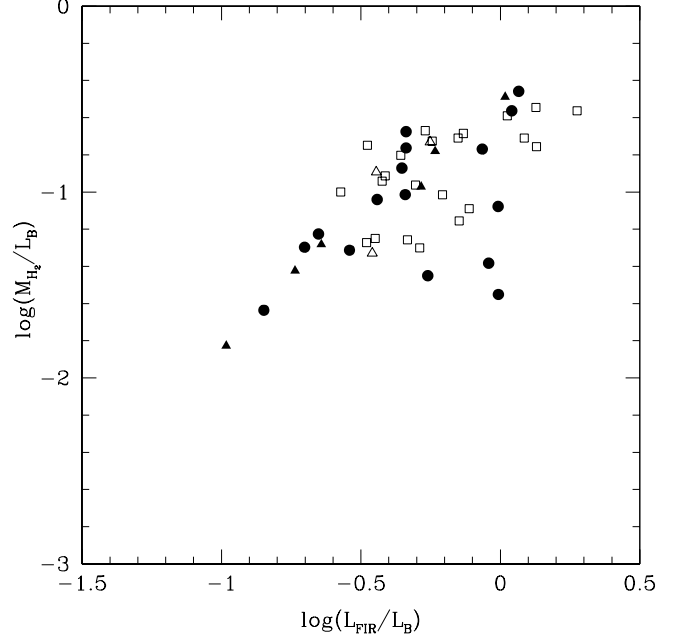

Fig. 4. Molecular gas normalized by blue luminosity as a function of FIR luminosity normalized by blue luminosity. The CS is marked by open symbols and HDS by filled symbols. LINERs are marked by triangles. Luminosities are in $L_\odot$ and mass in $M_\odot$.
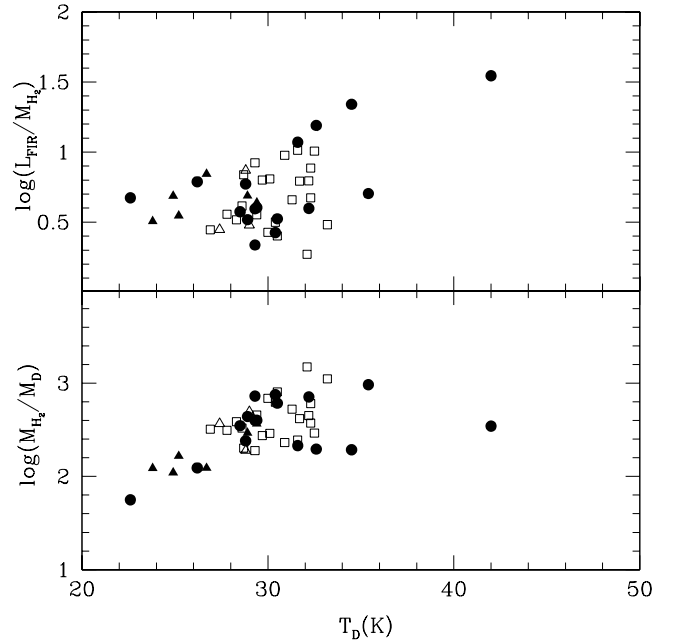

Fig. 5. Upper panel: FIR luminosity normalized by molecular gas as a function of dust temperature in K. Lower panel: molecular gas normalized by dust mass as a function of dust temperature in K. Luminosities are in $L_\odot$ and mass in $M_\odot$. Symbols are the same as in Fig. 4.

toriza et al. (1994) for galaxies in other subsamples of HDS and CS galaxies. The main difference between the latter subsample and our subsample is the morphology and type of activity. The majority of the galaxies in Pastoriza et al. (1994) with large EWs are either later type spirals or classical Seyfert galaxies, like NGC7582. In our subsample we have spirals of intermediate type and no Seyferts.

Since the HDS has more LINERs than the CS and LINERs tend to have smaller EW(Hα), we find that, if we disregard all LINERs, the mean value of EW(Hα) changes to 19.8 ± 10.1 and 15.3 ± 9.0Å, for the HDS and CS, respectively. However, the number of galaxies with measured EW(Hα) is too small to give any statistically significant result. SFRs based on L(Hα) can also be severely underestimated due to dust internal to the galaxies (Bushouse 1987, Kennicutt 1998). Therefore, we use L$_{FIR}$ as a diagnostic to the recent star formation.

3. Discussion

3.1. Environment

In order to investigate whether there is any correlation between the environment, the type of activity, and the total amount of molecular gas, we have identified galaxies in the HDS which are also part of groups according to Maia et al. (1989). As environmental parameters we used the number of companions and the mean separation between the galaxies of each group (N$_g$ and r$_p$ in Maia et al. 1989). We plotted M$_{H_2}$/L$_B$, EW(Hα) and SFE, as a function of N$_g$ and r$_p$ (Fig. 6, Fig. 7). We also marked in these figures the mean values for clusters of galaxies, starburst galaxies, and Hickson compact groups. No correlation between M$_{H_2}$/L$_B$ and the environmental parameters is found. There are galaxies as gaseous as starbursts and as poor as clusters in all environments. LINERs were found only in groups with less than 20 members but are present in groups with either small or large separations between the members.

We also found no correlation between EW(Hα) and the environmental parameters. This is in disagreement with Barton et al. (2000) who found that EW(Hα) anticorrelates strongly with pairs spatial separation and velocity separation. However, this could be either due to the small size of our sample in comparison with Barton et al. (2000) which contains 502 galaxies, and/or to the differences in the selection criterion imposed by our sample and Barton et al. The latter sample mixes pairs and groups of galaxies whereas our sample has galaxies in dense environments and no isolated pairs of galaxies.

The lack of a trend in Fig. 6 and Fig. 7 is clear. However, we decided to check some galaxies individualy. We noticed that three of the HDS galaxies (eso-lv1570050, eso-lv5450100, and eso-lv5480380) with the largest values of EW(Hα) have less M$_{H_2}$/L$_B$ than the average value. They are located in groups with small and large separations (e.g. r$_{peso-lv5450100}$=0.40 Mpc, r$_{peso-lv5480380}$=0.94
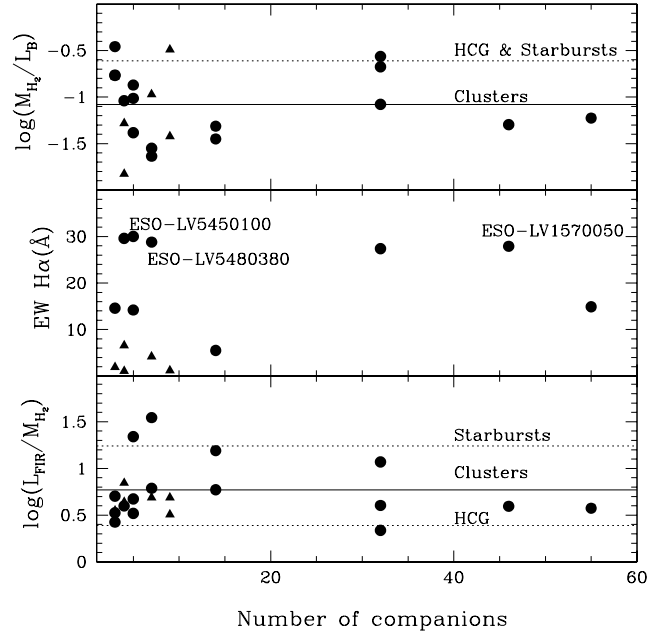

Fig. 6. Upper panel: Molecular gas normalized by blue luminosity as a function of the number of companions of galaxies (N$_g$) in the HDS. Middle panel: the equivalent width of Hα in Å as a function of N$_g$ in the HDS. Lower panel: FIR luminosity normalized by molecular gas as a function of N$_g$ in the HDS. Horizontal lines are average values for Hickson compact groups (HCG), starbursts and clusters from Leon et al. (1998). LINERs are marked by triangles. Luminosities are in L$_\odot$ and mass in M$_\odot$.

Mpc, and r$_{peso-lv1570050}$ = 1.3 Mpc) and with small and large number of companions (eso-lv5450100 has only 4 companions, eso-lv5480380 has 6 companions whereas eso-lv1570050 has 45 companions). Therefore, for these three galaxies, these environmental parameters are not responsible for the enhancement of star-formation and defficiency in molecular gas.

There is also no correlation between SFE and the environmental parameters. (Fig. 6 and Fig. 7 lower panels). Combes et al. (1994) also found no correlation between SFE and separation in pairs of galaxies. However, because pairs of galaxies are FIR enhanced they suggested that pairs have an increase in the molecular gas content. However, this is not the case for our sample. No clear trend between the environment and L$_{FIR}$/L$_B$ is found (Fig. 8). We note that the two galaxies with the largest number of companions have the lowest L$_{FIR}$/L$_B$. This could be an indication of the influence of the environment on the star formation rate of these galaxies and should be investigated for a larger sample. Similar results were suggested by Hashimoto et al. (1998) using the [OII] emission line as a diagnostic of SFR.

The possibility of a correlation with the crossing time (t$_v$ in Maia et al. 1989) was also checked and no correlation
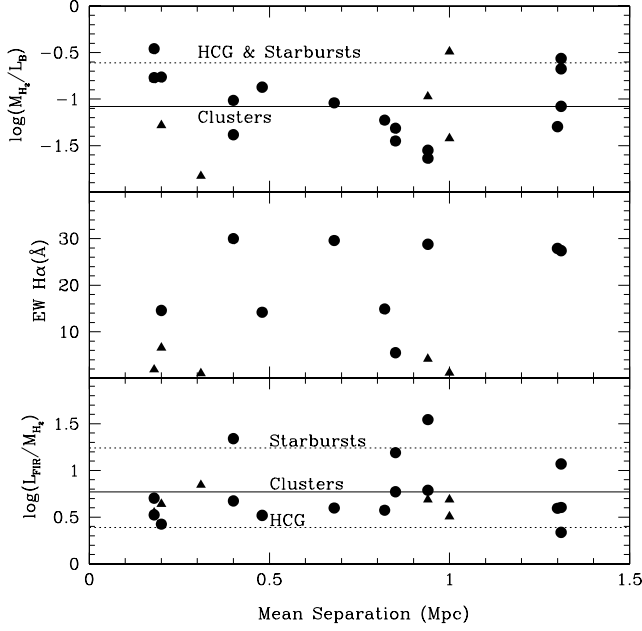
Fig. 7. Upper panel: Molecular gas normalized by blue luminosity as a function of the mean separation (r_p) between galaxies in the HDS. Middle panel: the equivalent width of Hα in Å as a function of r_p in the HDS. Lower panel: FIR luminosity normalized by molecular gas as a function of r_p in the HDS. Horizontal lines are for Hickson compact groups (HCG), starbursts and clusters from Leon et al. (1998). LINERs are marked by triangles. Luminosities are in $L_\odot$, mass in $M_\odot$, and r_p in Mpc.

was found. Therefore, we conclude that *there is no clear correlation between molecular gas content, SFR, SFE and the environmental parameters.*

3.2. Total Gas and Morphology

It is possible that interacting galaxies like galaxies in compact groups have less current star formation because they have less total fuel (Sulentic & de Mello Rabaça 1993, Leon et al. 1998). Therefore, the total amount of gas, H_2 + HI, might be a better SFE indicator in very dense environments. In order to check if this is valid for our sample, we used the HI data available in the NED for 35 galaxies of our sample. Our results are:

– **Total gas**: $(M_{HI}+M_{H_2})/L_B$ distributions (Fig. 9) are significantly different (91% level).
   The HDS has lower total gas than the CS.
– **Gas Fraction**: the average values of log (M_{HI}/M_{H_2}) for the HDS and CS are 0.69±0.59 and 0.51±0.46. M_{HI}/M_{H_2} distributions are significantly different (88% level).
   The HDS in comparison with CS have, more atomic gas, or higher atomic gas fraction. Similar values
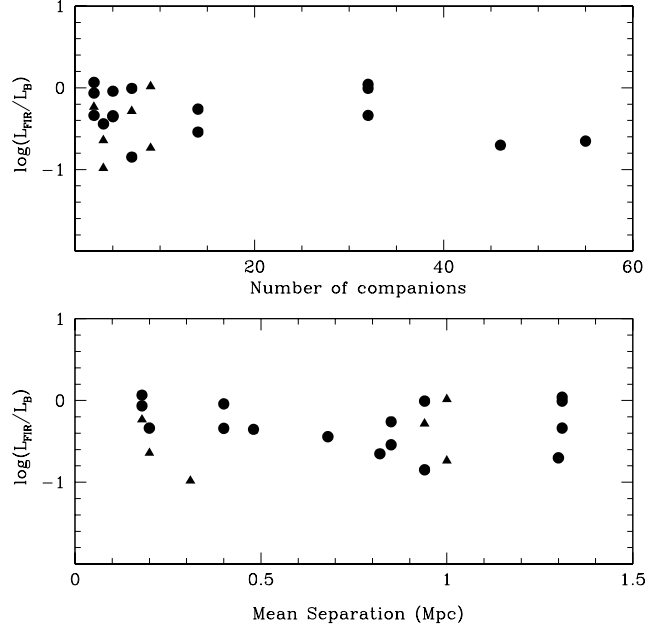
Fig. 8. Upper panel: Number of companions (N_g) of galaxies in the HDS as a function of FIR luminosity normalized by the blue luminosity. Lower panel: Mean separation (r_p) between the members of the groups in the HDS as a function of FIR luminosity normalized by the blue luminosity. LINERs are marked by triangles. Luminosities are in $L_\odot$ and r_p in Mpc.

(log (M_{HI}/M_{H_2})=0.62±0.43) are found by Horellou & Booth (1997) for a sample of southern interacting galaxies.

– **SFE (L_{FIR}/total gas)**: the star formation efficiency calculated using the total gas, $L_{FIR}/(M_{HI}+M_{H_2})$, distributions (Fig. 10) are not significantly different (55% level).

Fig. 11 shows the SFE indicators as a function of L_{FIR}/L_B (both plots include only galaxies for which HI data were available). The large dispersion seen in the upper panel decreases in the lower panel where we include the neutral gas. The correlation coefficient changes from 0.21 to 0.73 in the HDS and 0.59 to 0.46 in the CS (r in Table 3).

Fig. 12 shows the SFE including the atomic gas, $L_{FIR}/(M_{HI}+M_{H_2})$, as a function of the SFE without the atomic gas. The three most efficient galaxies previously found using only the molecular gas (eso-lv5480380, eso-lv5450100, eso-lv1190060) still have high values of SFE when we include the HI content. However, it is interesting to see how other galaxies (eso-lv3520530, eso-lv4050180, and eso-lv5480310 - marked in Fig. 12) which were not among the efficient ones, now have higher values. This could be due to the low amount of HI in these *earlier types spirals.* If we remove them from our sample and keep a more
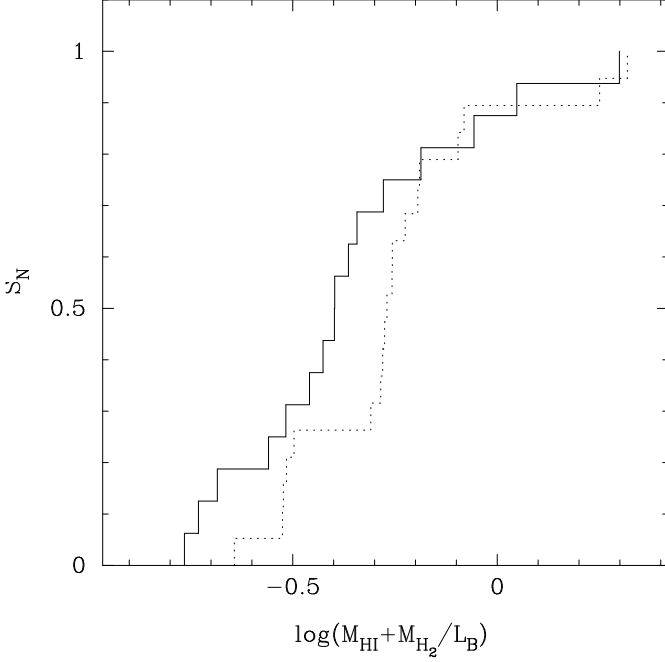
Fig. 9. Cumulative probability distribution of the total gas normalized by total gas. HDS is marked by solid line and CS by dotted line. Luminosity is in $L_\odot$ and mass in $M_\odot$.
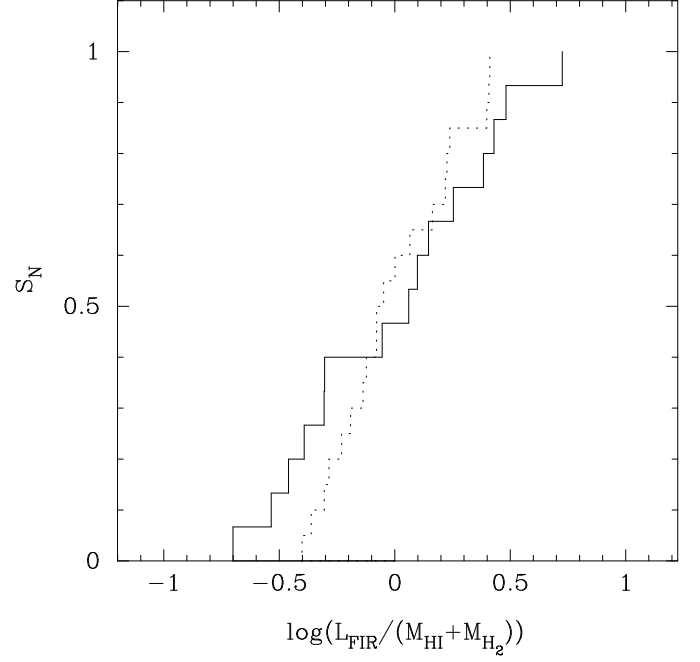

Fig. 10. Cumulative probability distribution of FIR luminosity normalized by total gas. HDS is marked by solid line and CS by dotted line. Luminosity is in $L_\odot$ and mass in $M_\odot$.

homogeneous sample in terms of morphology, we find that *log (M_{HI}/M_{H_2}) is higher for the HDS than for the CS.* The cumulative distribution function (Fig. 13) of the HDS is significantly different than that of the CS. However, we have HI data for only 12 galaxies of the HDS which are later than Sb, therefore, a larger and homogeneous sample in terms of morphology should be observed in order to confirm this result.

4. Summary and Conclusions

We have performed a detailed comparison between properties of intermediate Hubble type galaxies in dense environments (HDS) and in the field (CS). By using several different diagnostics of global properties we have found a trend for the gaseous content and star formation properties of the high and low density samples. Intermediate Hubble type galaxies in dense environments have, on average:

- **lower** gas content than field galaxies (i.e. lower M_{gas}/L_B ratio)
- **higher** atomic gas fraction than field galaxies (i.e. a higher M_{HI}/M_{H_2} ratio)
- **lower** current star formation rate than field galaxies (i.e. lower L_{FIR}/L_B ratio)
- the **same** star formation efficiency as field galaxies (i.e. the same L_{FIR}/M_{H_2} or L_{FIR}/M_{gas} ratio)
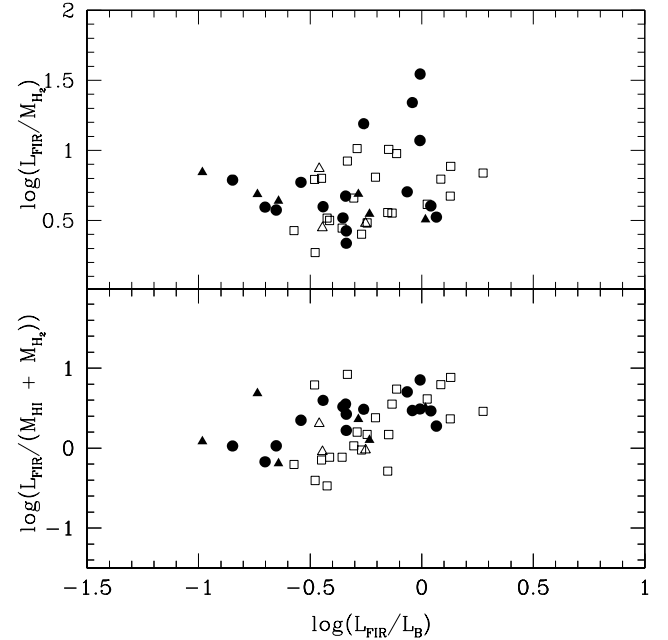

Fig. 11. Upper panel: FIR luminosity normalized by molecular gas as a function of FIR luminosity normalized by blue luminosity Lower panel: FIR luminosity normalized by total (neutral and molecular) gas as a function of FIR luminosity normalized by blue luminosity. Symbols are the same as in Fig. 4. Luminosities are in $L_\odot$ and mass in $M_\odot$.
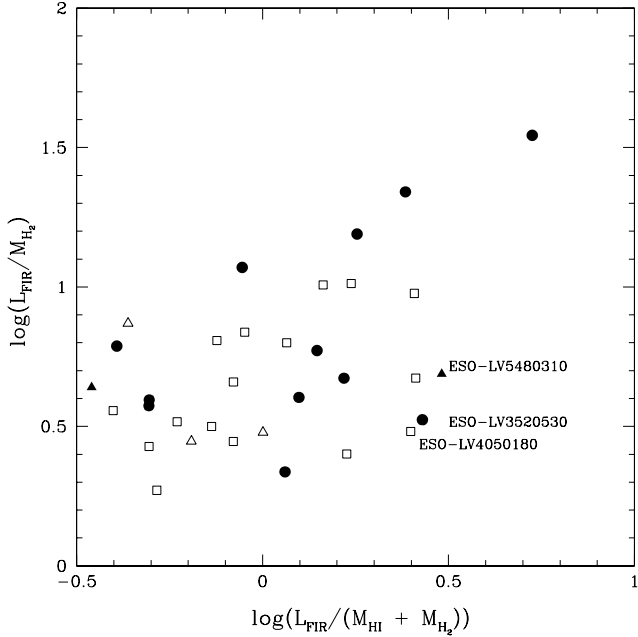
Fig. 12. FIR luminosity normalized by molecular gas as a function of FIR luminosity normalized by total (atomic and molecular) gas. Symbols are the same as in Fig. 4. Luminosities are in $L_\odot$ and mass in $M_\odot$.

Fig. 13. Cumulative probability distribution of atomic and molecular gas ratio. HDS is marked by solid line and CS by dotted line.

Although none of the above results stand out as a single strong diagnostic given their statistical significance (see Table 3), taken together they suggest a trend for diminished gas content and star formation activity in galaxies in high density environments.

What can be the physical processes behind this result? It has long been believed that gravitational interaction is a sufficient condition for transporting gas from the outer regions of galaxies to the inner regions, and thereby increasing the star formation activity. If this is the case for our high density sample, the lower gas content could be the result of gas exhaustion through an increased star formation activity *in the past*. However, it seems unlikely that we should have selected only those systems which experienced enhanced star formation rates in the past. An alternative and more likely interpretation is that repeated close encounters, experienced by galaxies in dense environments, removes gas from the galaxies as well as leads to an inhibition of the formation of molecular gas from the atomic phase. The similarities in star formation efficiency then suggest that the physical processes controling the formation of stars from the molecular gas are local rather than global.

In addition, we find that 6 (38%) of the HDS galaxies and 3 (14%) of the CS galaxies are classified as LINERS. These are very limited numbers but a few interesting trends among the LINERS are suggested by our data. First of all, the LINERS show a very good correlation
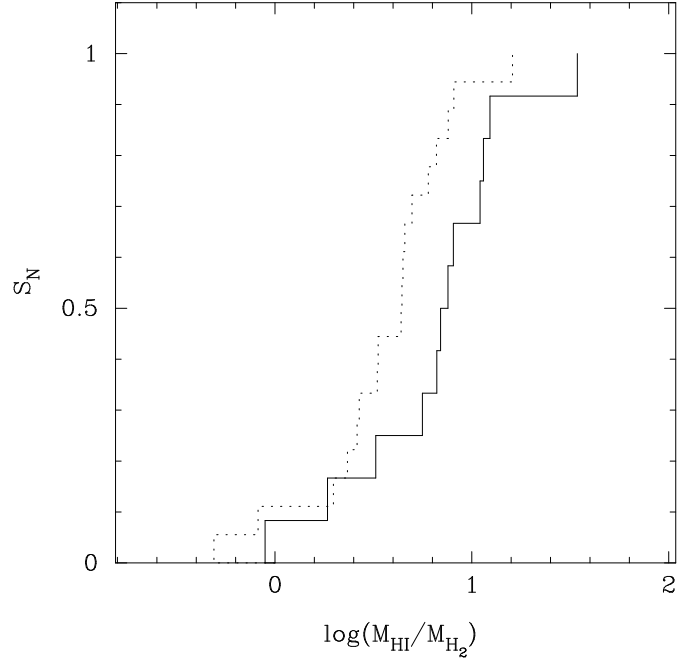
between molecular gas and L_{FIR}, they have a lower dust temperature than the non-LINER HDS and CS galaxies and they have a lower average star formation efficiency. These findings are consistent with the LINERS as aging starbursts rather than being powered by an AGN. A larger sample is needed to study these correlations in more detail.

References

Aaronson, M., Huchra, J., Mould, J., Schechter, P.L., & Tully, R.B. 1982, ApJ 258, 64

Alonso-Herrero, A., Rieke, M.J., Rieke, G.H., & Shields, J.C. 2000, ApJ 530, 688

Allam, S., Assendorp, R., Longo, G., Braun, M., & Richter, G. 1996, A&AS 117, 39

Baldwin, J.A., Phillips, M.M., & Terlevich, R. 1981, PASP 93, 5

Barton, E.J., Geller, M.J., & Kenyon, S.J. 2000, ApJ 530, 660

Boselli, A., Mendes de Oliveira, C., Balkowski, C., Cayatte, V., & Casoli, F. 1996, A&A 314, 738

Braine, J., Combes, F., Casoli, F., Dupraz, C., Gerin, M., Klein, U., Wielebinski, R., & Brouillet, N. 1993, A&AS 97, 88

Bushouse, H.A. 1987, ApJ 320, 49

Casoli, F., Boisse, P., Combes, F. & Dupraz, C. 1991, A&A 249, 359

Casoli, F., Dickey, J., Kazes, I., Boselli, A., Gavazzi, P., & Baumgardt, K. 1996, A&A 309, 43

Combes, F., Prugniel, P., Rampazzo, R., & Sulentic, J.W. 1994, A&A 281, 725

Coziol, R., Iovino, A., & de Carvalho, R.R. 2000, AJ 120, 47

da Costa, L.N., Pellegrini, P.S., Willmer, C., de Carvalho, R., Maia, M., Latham, D.W., & Geary, J.C. 1989, AJ 97, 315

Dahari, O. 1984, AJ 89, 966

de Mello, D.F., Maia, M.A.G., & Wiklind, T. 2001, A&A submitted (Paper I)

Gerin, M., & Casoli, F. 1994, A&A 290, 49

Hashimoto, Y., Oemler, A.Jr., Lin, H., & Tucker, D.L. 1998, ApJ 499, 589

Hickson, P. 1997, ARA&A 35, 357

Hildebrand, R.H. 1983, QJRAS, 24, 267

Ho, L.C., Filippenko, A.V., Sargent, W.L.W. 1997, ApJS 112, 315

Horellou, C., Casoli, F., Combes, F., & Dupraz, C. 1995, A&A 298, 743

Horellou, C., Booth, R. 1997, A&AS 126, 3

Huchtmeier, W.K. 1997, A&A 325, 473

Ji, L., Chen, Y., Huang, J.H., Gu, Q.S., & Lei, S.J. 2000, A&A 355, 922

Keel, W.C., Kennicutt, R.C.Jr., van der Hulst, J.K. & Hummel, E. 1985, AJ 90, 708

Keel, W.C. 1996, AJ 111, 696

Kenney, J.D.P., & Young, J.S. 1988, ApJ 326, 588

Kennicutt, R.C.Jr. 1983, ApJ 272, 54

Kennicutt, R.C.Jr. 1998, ARA&A 36, 189

Kennicutt, R.C.Jr., Bothun, G.D., & Schommer, R.A. 1984, AJ 89, 1279

Kennicutt, R.C.Jr., & Keel, W.C. 1984, ApJ 279, 5

Lauberts, A. 1982, The ESO/Uppsala Survey of the ESO(B) Atlas (Munich: European Southern Observatory)

Lauberts, A., & Valentijn, E.A. 1989, The Surphace Photometry Catalogue of the ESO-Uppsala Galaxies (Garching bei München: ESO)

Larson, R.B. & Tinsley, B.M. 1978, ApJ 219, 46

Leon, S., Combes, F., & Menon, T.K. 1998, AA, 330, 37

Liu, C.T., & Kennicutt, R.C.Jr. 1995, ApJ 450, 547

Maia, M.A.G., da Costa, L.N., & Latham, D.W. 1989, ApJS 69, 809

Maia, M.A.G., Pastoriza, M.G., Bica, E., & Dottori, H. 1994, ApJS 93, 425

Maia, M.A.G., Willmer, C.N.A., & da Costa, L.N. 1998, AJ 115, 49

Maiolino, R., Ruiz, M., Rieke, G.H., & Papadopoulos, P. 1997, ApJ 485, 552

Mendes de Oliveira, C., & Hickson, P. 1994, ApJ 427, 684

Mihos, J.C.,& Hernquist, L. 1994, ApJ 437, L47

Moshir, M. et al. 1990, IRAS Faint Source Catalogue, version 2.0.

Pastoriza, M.G., Bica, E., Maia, M.A.G., & Dottori, H. 1994, ApJ, 432, 128

Press, W.H., Flannery, B.P., Teukolsky, S.A., & Vetterling, W.T. 1989, Numerical Recipes, The Art of Scientific Computing (FORTRAN Version) Cambridge University Press

Roberts, M.S., & Haynes, M.P. 1994, ARA&A 32, 115

Sage, L.J. 1993, A&A 272, 123

Sanders, D.B., Scoville, N.Z., & Soifer, B.T. 1991, ApJ 370, 158

Sulentic, J.W., & de Mello Rabaça, D.F. 1993, ApJ 410, 520

Szomoru, A., van Gorkom, J.H., Gregg, M.D., & Strauss, M.A. 1996, AJ 111, 2150

Thronson, H.A., & Telesco, C.M. 1986, ApJ 311, 98

Veilleux, S., & Osterbrock, D.E. 1987, ApJS 63, 295

Young, J.S., & Knezek, P. 1989, ApJ 347, L55

Young, J.S., Shuding, X., Kenney, J.D.P. et al. 1989, ApJS 70, 699

Wiklind, T., Combes, F., & Henkel, C. 1995, A&A 297, 643

Williams, B.A., & Rood, H.J. 1987, ApJS 63, 265